

## Spectral Analog of the Gouy Phase Shift

Esben Ravn Andresen,<sup>1</sup> Christophe Finot,<sup>2</sup> Dan Oron,<sup>3</sup> and Hervé Rigneault<sup>1,\*</sup>

<sup>1</sup>*Institut Fresnel, CNRS, Aix-Marseille Université, Ecole Centrale Marseille, Campus de Saint Jérôme, F-13397 Marseille Cedex 20, France*

<sup>2</sup>*Laboratoire Interdisciplinaire Carnot de Bourgogne, CNRS, Université de Bourgogne, 9 Avenue Alain Savary, 21078 Dijon, France*

<sup>3</sup>*Department of Physics of Complex Systems, Weizmann Institute of Science, Rehovot 76100, Israel*

(Received 13 November 2012; published 3 April 2013)

We demonstrate the existence of the spectral phase shift a pulse experiences when it is subjected to spectral focusing. This  $\frac{\pi}{2}$  phase shift is the spectral analog of the Gouy phase shift a 2D beam experiences when it crosses its focal plane. This spectral Gouy phase shift is measured using spectral interference between a reference pulse and a negatively chirped parabolic pulse experiencing spectral focusing in a nonlinear photonic crystal fiber. To avoid inherent phase instability in the measurement, both reference and parabolic pulses are generated with a 4- $f$  pulse shaper and copropagate in the same fiber. We measure a spectral phase shift of  $\frac{\pi}{2}$ , reaffirming its generality as a consequence of wave confinement in the spatial, temporal and spectral domains.

DOI: 10.1103/PhysRevLett.110.143902

PACS numbers: 42.25.Bs, 42.65.Jx, 42.81.Dp

In 1890 Louis-Georges Gouy [1] reported for the first time the existence of an extra phase contribution  $\phi_G$  to the propagative phase  $kz$  ( $k$  being the wave vector and  $z$  the distance) a beam experiences when it travels through its focus. Besides its experimental demonstration, Gouy could explain the phase advance postulated by Fresnel for the secondary Huygens wavelets created from a primary wave front in wave diffraction theory [2]. Although the Gouy phase anomaly is well described by Maxwell wave propagation theory, there have been several attempts to give a more intuitive description of this phenomenon [3–5]. As already noted by Gouy, this phase anomaly exists for any and all waves and is equal to  $\phi_G = \frac{\pi}{2}$  for each dimension of transverse confinement: a 3D beam having a 2D wave front thus experiences a  $\phi_G^{\text{space}}$  of  $\pi$  when crossing its focus whereas a 2D beam having a 1D wave front experiences a  $\phi_G^{\text{space}}$  of only  $\frac{\pi}{2}$ . The analogy between spatial diffraction and temporal dispersion has been known for many years [6,7]. This space-time duality is due to the mathematically identical equations describing spatial and temporal wave propagation [8] and many diffractive optical elements have temporal analogs that perform parallel functions in the time domain [9]. Considering the simple case of a cylindrical lens with a focal length  $f$  (we restrict here our analysis to 1D for simplicity and adopt an  $e^{-i\omega T}$  field time dependence), the well-known spatial focusing arises from successively imposing onto a 2D field a quadratic phase  $e^{-i(k/2f)x^2}$  in real space and a quadratic phase  $e^{-i(d/2k)k_x^2}$  in momentum space, representing a lens and propagation over a distance  $d$  to the focus, respectively, [Fig. 1(a)]. As described above, this 1D spatial confinement is accompanied by the spatial Gouy phase  $\phi_G^{\text{space}} = \frac{\pi}{2}$ .

As a spatial lens imposes a quadratic phase in space  $x$ , a time lens shall produce a quadratic phase in time  $t$ . This

can be done with a phase modulator or by self phase modulation (SPM) acting on a parabolic pulse [10]. As a consequence, and analogously to a spatial lens, a pulse can be confined in time by imposing a temporal quadratic

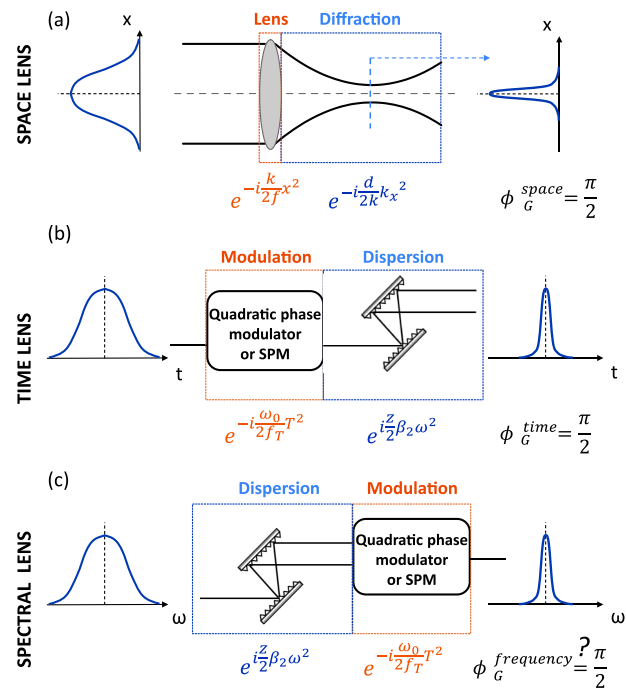


FIG. 1 (color online). Space, time, and spectral lenses. (a) Spatial confinement arises from successively imposing a quadratic phase in real space and in  $k$  space and the spatial phase experiences a  $\pi/2$  Gouy phase shift. (b) Time confinement arises from successively imposing a quadratic phase in time and in frequency and the temporal phase experiences a  $\pi/2$  phase shift. (c) Spectral confinement arises from successively imposing a quadratic phase in frequency and in time, and it raises the question of the existence of a  $\pi/2$  spectral phase shift.

phase ( $e^{-i(\omega_0/f_T)T^2}$ ) followed by a quadratic phase in frequency ( $e^{i(z\beta_2/2)\omega^2}$ ) [Fig. 1(b)], the latter representing nothing but a dispersive delay line. In the above written expressions  $f_T = \frac{\omega_0}{d^2\phi(T)/dT^2}$  is the focal time ( $\phi$  being the phase),  $\omega_0$  the pulse central frequency,  $\beta_2 = \frac{d^2\beta}{d\omega^2}$  ( $\beta$  is the propagation constant along  $z$ ),  $T$  and  $z$  are the time and spatial variables in the traveling-wave coordinate system (traveling at the pulse group velocity), respectively [8]. Quite interestingly this confinement in time is also accompanied by a phase shift  $\phi_G^{\text{time}}$  besides the propagative phase  $-\omega_0 T$  and it is analytically shown in textbooks that  $\phi_G^{\text{time}} = \frac{\pi}{2}$  for a temporal Gaussian pulse propagating in a linear dispersive medium [11].  $\phi_G^{\text{time}}$  could be appropriately named the “temporal Gouy phase” because the equations describing the evolution in time of a (temporal) Gaussian pulse in a dispersive medium are mathematically equivalent to the ones describing the evolution in space of a (spatial) Gaussian pulse, both acquire a phase shift  $\phi_G^{\text{time}}$  ( $\phi_G^{\text{space}}$ ) as they cross their time (space) confinement point.

Less known than spatial and temporal confinement, spectral confinement is also possible [12]. A spectral lens is nothing but a quadratic phase in frequency  $e^{i(z\beta_2/2)\omega^2}$  followed by a temporal quadratic phase  $e^{-i(\omega_0/f_T)T^2}$  [Fig. 1(c)]. Such a spectral confinement is usually achieved with a dispersive delay line followed by SPM. SPM imposes a phase shift proportional to the temporal intensity envelope, so the best confinement is reached for a parabolic pulse which acquires the desired  $T^2$ -dependent phase when subjected to SPM. This way the pulse spectrum narrows, reaching a minimal value at the spectral focal plane and then broadens upon further propagation. Spectral focusing is often named spectral compression or spectral narrowing in the literature [13–15]. The “momentum lens” is missing from our discussion to complete the general picture of the Gouy phase shift in all direct and inverse space-time coordinates. The momentum lens is, however, trivially realized by inverting lens and free-space propagation in Fig. 1(a).

Everything is now in place to address the following question: Is there a spectral phase shift  $\phi_G^{\text{frequency}}$  on the spectral phase when a pulse experiences spectral focusing? Following the space-time analogy described earlier  $\phi_G^{\text{frequency}}$  should be appropriately named the “spectral Gouy phase” and its value is expected to be  $\frac{\pi}{2}$  as spectral focusing proceeds in 1D. It is the aim of this Letter to address this question both experimentally and theoretically.

To generate the analog of the Gouy phase in the spectral domain we use the experimental setup sketched in Fig. 2. The laser is a SESAM-modelocked laser (t-Pulse, Amplitude Systems, 50 MHz,  $\lambda_0 = 1035$  nm, 150 fs) which emits a pulse  $A_{\text{laser}}$  ( $A$  denotes the complex field and  $\tilde{A}$  its Fourier transform); a standard 4- $f$  pulse shaper [16] with a double 320-pixel liquid-crystal stripe array (SLM-320b, JenOptik) multiplies the transfer function

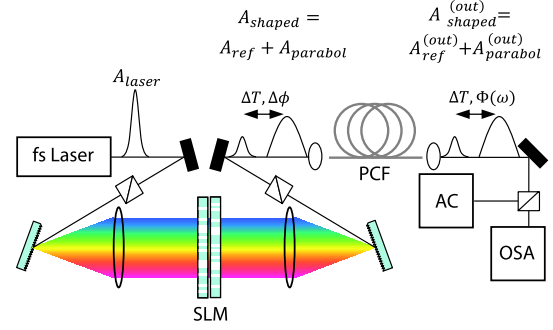


FIG. 2 (color online). Sketch of the experimental setup. SLM, spatial light modulator; AC, autocorrelator; optical spectrum analyzer, optical spectrum analyzer.

$H(\omega)$  on  $\tilde{A}_{\text{laser}}(\omega)$ , resulting in the shaped field  $\tilde{A}_{\text{shaped}}(\omega)$ .  $A_{\text{shaped}}$  is then launched into a 155 cm long photonic crystal fiber (PCF). The PCF output  $A_{\text{shaped}}^{(\text{out})}$  is characterized by a background-free autocorrelator and an optical spectrum analyzer. Before performing the experiment,  $|\tilde{A}_{\text{laser}}(\omega)|^2$  was measured and was found to be well described by a  $\text{sech}^2$ -function with a full width at half maximum (FWHM) of 8 nm. To compensate for residual dispersion of the optical elements before the PCF, the pulse shaper was programmed with the transfer function that gave a transform-limited  $A_{\text{laser}}(T)$  just before the PCF as verified by autocorrelation. This transfer function was added as an offset to all the transfer functions used in the following. Due in part to diffraction on the pixelized spatial light modulator (SLM) [17], in part to space-time coupling [18] and subsequent focusing by the PCF coupling lens [19,20], the combined system of pulse shaper and PCF exhibits a limited time window  $w(T)$ . In other words, the coupling efficiency into the PCF of a certain part of  $A_{\text{shaped}}$  depends on its time coordinate  $T$ .  $w(T)$  was determined by programming the pulse shaper with a delay  $H(\omega) = \exp(i\omega T)$  and recording  $\int |\tilde{A}_{\text{shaped}}(\omega)|^2 d\omega$  versus  $T$ . We found that  $w(T)$  was well described by a Gaussian with a FWHM of 3340 fs.  $w(T)$  was finally normalized for further use. In analogy with spatial focusing, we would like to measure the phase of the output pulse as a function of propagation distance (and hence degree of spectral compression) in the PCF. We work, however, with a PCF of fixed length, and hence choose to change the amount of nonlinear phase accumulated by SPM by changing the input power at a fixed fiber length.

We make an ansatz for the negatively chirped parabolic pulse to be generated by the pulse shaper

$$A_{\text{parabol}}(T) = \begin{cases} \sqrt{P_p} \sqrt{1 - \frac{T^2}{T_p^2}} e^{i\alpha T^2} & -1 \leq T/T_p \leq 1 \\ 0 & \text{otherwise} \end{cases}, \quad (1)$$

where  $P_p$  is the peak power,  $T_p$  the half full-width of  $|A_{\text{parabol}}(T)|^2$ , and  $\alpha$  the chirp parameter. For simplicity

the carrier frequency is set to zero. In practice, we pad the leading and trailing edge of  $A_{\text{parabol}}(T)$  with Gaussian tails at the FWHM to avoid discontinuities in its derivative. In the experiments, we used  $T_p = 1414$  fs and  $\alpha = 3 \times 10^{-6}$  fs $^{-2}$ . The Fourier transform of  $A_{\text{parabol}}(T)$  [normalized to  $w(T)$  and  $\sqrt{P_p}$ ],  $\tilde{A}_{\text{parabol}}(\omega) = \text{FT}^{-1}[w(T)^{-1}A_{\text{parabol}}(T)P_p^{-1/2}]$  is then computed and the required transfer function is found as

$$H_{\text{parabol}}(\omega) = \frac{\tilde{A}_{\text{parabol}}(\omega)}{\tilde{A}_{\text{laser}}(\omega)}. \quad (2)$$

When we program the pulse shaper with  $H_{\text{parabol}}$  a negatively chirped parabolic pulse  $A_{\text{parabol}}$  is thus generated. In order to measure the phase shift incurred by  $A_{\text{parabol}}$  during the propagation through the PCF, we generate a weak reference pulse  $A_{\text{ref}}$  which is a replica of  $A_{\text{laser}}$  delayed by  $\Delta T$  and phase shifted by  $\Delta\phi$  with respect to  $A_{\text{parabol}}$  and whose transfer function is

$$H_{\text{ref}}(\omega) = C_{\text{ref}} e^{i\omega\Delta T + i\Delta\phi}. \quad (3)$$

$C_{\text{ref}}$  and  $\Delta t$  were kept constant at 0.20 and 1414 fs throughout. Note that  $A_{\text{ref}}$  was kept sufficiently weak to avoid nonlinear effects occurring during its propagation in the PCF. Furthermore  $\Delta T$  was chosen long enough to avoid any interaction with  $A_{\text{parabol}}$  within the PCF [21].

The experiment proceeds as follows. We launch  $A_{\text{shaped}} = A_{\text{ref}} + A_{\text{parabol}}$  into the PCF. The field at the output of the PCF is  $A_{\text{shaped}}^{(\text{out})} = A_{\text{ref}}^{(\text{out})} + A_{\text{parabol}}^{(\text{out})}$  where  $A_{\text{parabol}}^{(\text{out})}$  has experienced spectral focusing and a possible spectral Gouy phase shift. The two are inherently phase stabilized as they are generated together by the SLM.  $A_{\text{parabol}}^{(\text{out})}$  and  $A_{\text{ref}}^{(\text{out})}$  interfere on the optical spectrum analyzer and from the spectral interference fringes, their relative phase  $\Phi(\omega)$  is determined. In practice, to minimize artifacts, the spectral interference is measured for 16 equidistant values of  $\Delta\phi$  and  $\Phi(\omega)$  is found from a sinusoidal fit to the 16 points at every wavelength in the spectrum. This was done for several different input powers  $P_p$  from which the dependence of  $\Phi(\omega)$  upon  $P_p$  was determined. Note that  $A_{\text{ref}}$  is the same throughout all the experiments so that, after having propagated through the PCF, the output pulse,  $A_{\text{ref}}^{(\text{out})}$  does not change its phase between experiments.

The calculations of pulse propagation in the PCF were done using a nonlinear Schrödinger equation (NLSE) assuming no loss, instantaneous nonlinearity and dispersion up to fifth order [22]. The solid core silica PCF had a core size of 2.5  $\mu\text{m}$  surrounded by a hexagonal hole pattern (hole size of 200 nm with a pitch of 1  $\mu\text{m}$ ). The exact value of the PCF nonlinearity parameter  $\gamma$  was unknown, but a reasonable value of  $\gamma = 0.047$  (W m) $^{-1}$  was assumed. The measured PCF dispersion curve was fitted by a fourth-order polynomial [23].

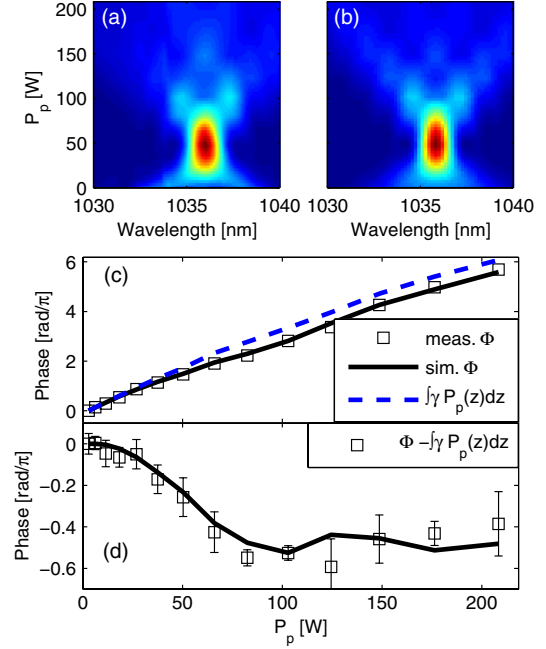


FIG. 3 (color online). Comparison of experimental and calculated results. (a) Measured PCF output spectra versus intrafiber peak power; (b) simulation of PCF output parameters using the same parameters as the experiment; (c) (open square) the measured relative phase  $\Phi(\omega_0)$  between parabolic pulse and reference pulse ( $\omega_0$  is the pulse central frequency); (solid line) the calculated relative phase using the same parameters as the experiment; and (dashed line) the propagative phase obtained from the calculations; (d) same as (c) but with the propagative phase subtracted. Pulse parameters:  $T_p = 1414$  fs;  $\alpha = -0.000003$  fs $^{-2}$ . PCF parameters:  $\gamma = 0.047$  (W m) $^{-1}$ ;  $L = 1.55$  m. The error bars denote one standard deviation.

The results of the experiments and comparison with the model are shown in Fig. 3. In Fig. 3(a) is presented the measured  $|\tilde{A}_{\text{parabol}}^{(\text{out})}(\omega)|^2$  versus  $P_p$  and in Fig. 3(b) a numerical simulation of the same using the same parameters as in the experiment. The agreement between measured and calculated spectra is excellent. The optimal focus is obtained for  $P_p = 50$  W where the spectrum is focused to a width FWHM of  $\sim 2$  nm—a fourfold narrowing. For  $P_p$  greater than 50 W the spectral focus is inside the PCF. The measured  $\Phi(\omega_0)$  at the central frequency  $\omega_0 = 2\pi c/\lambda_0$  of  $\tilde{A}_{\text{parabol}}^{(\text{out})}$  is plotted in Fig. 3(c) (squares) versus  $P_p$ ; the calculated phase extracted from the calculation is also shown (solid line). Once again, excellent agreement is found. We see that both increase almost linearly with  $P_p$  as expected in view of the solution of the NLSE. We remind readers that the solution to the NLSE in absence of dispersion is [11]

$$A(L, T) = A(0, T) e^{i\phi_{nl}}, \quad (4)$$

where the so-called nonlinear phase  $\phi_{nl} = \gamma P_p L$ , which would produce a straight line in Fig. 3(c). However, in the

presence of dispersion, the peak power of the pulse progressively changes and the expression must be modified to  $\phi_{nl} = \int \gamma P_p(z) dz$ . We infer  $P_p(z)$  from the calculation, use it to calculate  $\phi_{nl}$ , and plot it in Fig. 3(c) (blue or dashed line).  $\phi_{nl}$  does not take into account spectral confinement effects and, indeed, it is clearly seen that the  $\phi_{nl}$  cannot account for the entire phase shift incurred by the pulse in the PCF. To make the supplementary phase shift stand out more clearly, in Fig. 3(d) we plot the measured phase  $\Phi(\omega_0)$  minus  $\phi_{nl}$  (squares) as well as the simulated phase minus  $\phi_{nl}$  (black or solid line). A phase jump of  $\pi/2$  is accumulated between  $P_p = 30$  W and  $P_p = 70$  W, which is the power value range for which the spectrum comes to a focus in Figs. 3(a) and 3(b). This phase jump, denoted  $\phi_G^{\text{frequency}}$ , is the spectral analogue of the Gouy phase shift and arises as a result of the 1D spectral confinement.

To gain insight into the origin of  $\phi_G^{\text{frequency}}$  and how it develops let us consider the NLSE in the absence of loss and dispersion  $\frac{\partial A(z, T)}{\partial z} = i\gamma |A(z, T)|^2 A(z, T)$ . For simplicity let us consider a transform-limited parabolic field intensity  $|A(z, T)|^2 = P_p(1 - \frac{T^2}{T_p^2})$ , where  $P_p$  and  $T_p$  are the pulse power and width. The NLSE reads

$$\frac{\partial A(z, T)}{\partial z} = \frac{i}{L_{nl}} A(z, T) - \frac{i}{L_{nl} T_p^2} T^2 A(z, T), \quad (5)$$

where  $L_{nl} = \frac{1}{\gamma P_p}$  is the nonlinear length. The first right-hand side term of Eq. (5) stands for the nonlinear propagative phase responsible for the straight line in Fig. 3(c) [ $A(z, T) = A(0, T)e^{i\gamma P_p z}$ ] whereas the second term imposes a temporal quadratic phase modulation on the incoming field amplitude  $A(z, T) = A(0, T)e^{-(iT^2 z)/(L_{nl} T_p^2)}$  as sketched in Fig. 1(c). We aim now at deriving the spectral amplitude evolution

$$\tilde{A}(z, \omega) = \int_{-\infty}^{+\infty} A(0, T) e^{i\omega T - (iT^2 z)/(L_{nl} T_p^2)} dT \quad (6)$$

as the field propagates down the fiber. In order to pursue the analytical derivations, we consider an incoming Gaussian pulse  $\tilde{A}(0, \omega) = e^{-\omega^2/(2\Gamma_0^2)}$  with  $\Gamma_0$  the half width at  $1/e$  intensity. While not equivalent to the experiment in which a parabolic pulse was employed, the situation considered in the model could be achieved experimentally by letting a weak, Gaussian pulse copropagate with a perpendicularly polarized strong, parabolic pulse. Because we have considered a transform-limited Gaussian pulse, the spectral focusing arises at  $z = 0$  in this simple parabolic model. The spectral divergence from the spectral focus is then found by propagation of  $\tilde{A}(0, \omega)$  and the spectral convergence up to the focus by backpropagation. Inserting the Fourier transform  $A(0, T) = \frac{\Gamma_0}{\pi\sqrt{2}} e^{-\Gamma_0 T^2/2}$  of  $\tilde{A}(0, \omega)$  into Eq. (6) and performing some algebra one obtains

$$\tilde{A}(z, \omega) = \frac{1}{(1 + i\frac{z}{L_s})^{1/2}} e^{-\omega^2/[2\Gamma_0^2(1 + iz/L_s)]}, \quad (7)$$

an expression very similar to the ones that are derived in textbooks in the case of a focused paraxial Gaussian beam (space domain) or the temporal confinement of a Gaussian beam (time domain). In Eq. (7)  $L_s = \Gamma_0^2 T_p^2 L_{nl}/2$  can be viewed as the spectral focusing length and plays a similar role to the Rayleigh length in the space domain. Rewriting Eq. (7) in amplitude and phase gives

$$\tilde{A}(z, \omega) = \sqrt{\frac{\Gamma_0}{\Omega(z)}} e^{-\omega^2/[2\Omega^2(z)]} e^{i\phi(z, \omega)} \quad (8)$$

with  $\Omega(z) = \Gamma_0(1 + \frac{z^2}{L_s^2})^{1/2}$  and

$$\phi(z, \omega) = \frac{\omega^2}{2\Omega^2(z)} \frac{z}{L_s} - \frac{1}{2} \arctan\left(\frac{z}{L_s}\right). \quad (9)$$

The amplitude of  $\tilde{A}(z, \omega)$  remains Gaussian throughout the propagation with  $\Omega(z)$  being the ‘‘spectral waist’’. After a propagation over  $z = L_s$  the half width at  $1/e$  intensity is  $\sqrt{2}\Gamma_0$  and while propagating further to  $z = +\infty$  the beam expands with a spectral divergence  $\theta_{\text{spec}} = \frac{\Gamma_0}{L_s}$ . The phase shows a quadratic dependence in  $\omega$  indicating that the beam is rapidly chirped after the spectral focus at  $z = 0$ . The second right-hand side term in Eq. (9) is the spectral Gouy phase shift  $\phi_G^{\text{frequency}} = -\frac{1}{2} \arctan(\frac{z}{L_s})$  and amounts to a  $\pi/2$  jump when the beam travels from  $z = -\infty$  to  $+\infty$ . In practice, and as their space and time counterparts, the  $\pi/2$  spectral Gouy phase shift is accumulated between  $z = -L_s$  and  $z = +L_s$ .

From simple analogies between the spatial focusing of light and the temporal confinement a pulse experiences when it is subjected to dispersion, we have addressed the question of the existence of a spectral analog of the Gouy phase shift in spectral focusing. Using a 4-*f* pulse shaper to generate a negatively chirped parabolic pulse together with a weak reference pulse, we have been able to measure the phase change a beam experiences when it is spectrally focused in a nonlinear optical fiber. Our experiment reveals that, on top of the nonlinear phase, a phase shift anomaly  $\phi_G^{\text{frequency}}$  exists that is equal to  $\frac{\pi}{2}$ . The measurements were found in good agreement with the numerical solution of the nonlinear Schrödinger equation. Furthermore, the analytical derivation of the interaction between a strong parabolic pulse and a weak Gaussian pulse revealed that  $\phi_G^{\text{frequency}}$  develops over a distance  $L_s$  that plays a similar role to the Rayleigh distance in spatial focusing. Our findings demonstrate that the Gouy phase shift is in no way uniquely associated with linear propagation since spectral focusing follows nonlinear propagation; it is a general feature of wave confinement in some direct or inverse coordinate, whether spatial or temporal.

We thank Jonathan C. Knight, Bath University, for supplying the PCF. We are grateful to Amplitude Systems for making the t-Pulse laser available for the measurements. The authors acknowledge the financial support from the Centre National de la Recherche Scientifique (CNRS) Weizmann NaBi European Associated Laboratory, the High Council for Scientific and Technological Cooperation between France-Israel (2012 Grant), the French Research Agency (ANR grant SOFICARS), and the Region Provence Alpes Cote d'Azur.

---

\*Corresponding author.

herve.rigneault@fresnel.fr

- [1] L. G. Gouy, C. R. Acad. Sci. Paris Ser. IV **110**, 1251 (1890).
- [2] M. Born and E. Wolf, *Principles of Optics* (Pergamon Press, New York, 1980).
- [3] R. W. Boyd, *J. Opt. Soc. Am.* **70**, 877 (1980).
- [4] S. Feng and H. G. Winful, *Opt. Lett.* **26**, 485 (2001).
- [5] T. D. Visser and E. Wolf, *Opt. Commun.* **283**, 3371 (2010).
- [6] A. Papoulis, *Systems and Transforms with Applications in Optics* (McGraw-Hill, New York, 1968), p. 200.
- [7] S. A. Akhmanov, A. P. Sukhorukov, and A. S. Chirkin, *Sov. Phys. JETP* **28**, 748 (1969).
- [8] B. H. Kolner, *IEEE J. Quantum Electron.* **30**, 1951 (1994).
- [9] J. van Howe and C. Xu, *J. Lightwave Technol.* **24**, 2649 (2006).
- [10] B. H. Kolner and M. Nazarathy, *Opt. Lett.* **14**, 630 (1989).
- [11] G. P. Agrawal, *Nonlinear Fiber Optics* (Academic Press, San Diego, 2001), 3rd ed., p. 68, Eq. 3.2.12.
- [12] R. H. Stolen and C. Lin, *Phys. Rev. A* **17**, 1448 (1978).
- [13] S. A. Planas, N. L. Pires Mansur, C. H. Brito Cruz, and H. L. Fragnito, *Opt. Lett.* **18**, 699 (1993).
- [14] E. R. Andresen, J. M. Dudley, C. Finot, D. Oron, and H. Rigneault, *Opt. Lett.* **36**, 707 (2011).
- [15] J. Fatome, B. Kibler, E. R. Andresen, H. Rigneault, and C. Finot, *Appl. Opt.* **51**, 4547 (2012).
- [16] A. M. Weiner, *Rev. Sci. Instrum.* **71**, 1929 (2000).
- [17] M. M. Wefers and K. A. Nelson, *J. Opt. Soc. Am. B* **12**, 1343 (1995).
- [18] J. Paye and A. Migus, *J. Opt. Soc. Am. B* **12**, 1480 (1995).
- [19] B. J. Sussman, R. Lausten, and A. Stolow, *Phys. Rev. A* **77**, 043416 (2008).
- [20] F. Frei, A. Galler, and T. Feurer, *J. Chem. Phys.* **130**, 034302 (2009).
- [21] E. R. Andresen, J. Dudley, D. Oron, C. Finot, and H. Rigneault, *J. Opt. Soc. Am. B* **28**, 1716 (2011).
- [22] G. P. Agrawal, *Nonlinear Fiber Optics* (Academic Press, San Diego, 2001).
- [23] Polynomial coefficients:  $\beta_2 = 18510 \text{ fs}^2/\text{m}$ ;  $\beta_3 = -53000 \text{ fs}^3/\text{m}$ ;  $\beta_4 = 194000 \text{ fs}^4/\text{m}$ ;  $\beta_5 = -351800 \text{ fs}^5/\text{m}$ ; and  $\beta_6 = 291800 \text{ fs}^6/\text{m}$ .